BIOCHEMISTRY
including biophysical chemistry & molecular biology

Article

pubs.acs.org/biochemistry

The Single-Giant Unilamellar Vesicle Method Reveals Lysenin-Induced Pore Formation in Lipid Membranes Containing Sphingomyelin

Jahangir Md. Alam,[†] Toshihide Kobayashi,[‡] and Masahito Yamazaki*[,†,§]

[†]Integrated Bioscience Section, Graduate School of Science and Technology, Shizuoka University, Shizuoka 422-8529, Japan

[‡]Lipid Biology Laboratory, RIKEN, Saitama 351-0198, Japan

[§]Department of Physics, Faculty of Science, Shizuoka University, Shizuoka 422-8529, Japan

Supporting Information

ABSTRACT: Lysenin is a sphingomyelin (SM)-binding pore-forming toxin. To reveal the interaction of lysenin with lipid membranes, we investigated lysenin-induced membrane permeation of a fluorescent probe, calcein, through dioleoylphosphatidylcholine (DOPC)/SM, DOPC/SM/cholesterol (chol), and SM/chol membranes, using the single-giant unilamellar vesicle (GUV) method. The results clearly show that lysenin formed pores in all the membranes, through which membrane permeation of calcein occurred without disruption of GUVs. The membrane permeation began stochastically, and the membrane permeability coefficient increased over time to reach a maximum, steady value, P^s, which persisted for a long time (100−500 s), indicating that the pore concentration increases over time and finally reaches its steady value, N_P^s. The P^s values increased as the SM/lysenin ratio decreased, and at low concentrations of lysenin, the P^s values of SM/DOPC/chol (42/30/28) GUVs were much larger than those of SM/DOPC (58/42) GUVs. The dependence of P^s on the SM/lysenin ratio for these membranes was almost the same as that of the fraction of sodium dodecyl sulfate (SDS)-resistant lysenin oligomers, indicating that N_P^s increases as the SDS-resistant oligomer fraction increases. On the other hand, lysenin formed pores in GUVs of SM/chol (60/40) membrane, which is in a homogeneous liquid-ordered phase, indicating that the phase boundary is not necessary for pore formation. The P^s values of SM/chol (60/40) GUVs were smaller than those of SM/DOPC/chol (42/30/28) GUVs even though the SDS-resistant oligomer fractions were similar for both membranes, suggesting that not all of the oligomers can convert into a pore. On the basis of these results, we discuss the elementary processes of lysenin-induced pore formation.

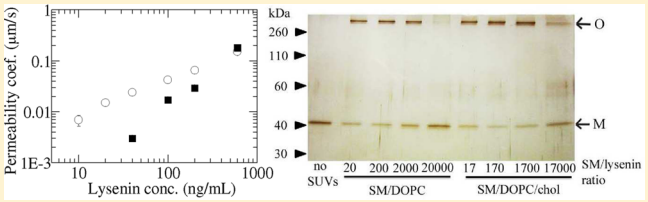

Pore-forming toxins (PFTs) have been discovered in, and isolated from, a wide variety of organisms, including bacteria and invertebrates.[1−4] The target of most of these protein toxins is considered to be lipid membrane regions of plasma membranes; water-soluble toxins bind to the plasma membrane and then create pores in the membrane that induce cytolysis. For example, α-hemolysin from *Staphylococcus aureus*,[5] pneumolysin from *Streptococcus pneumoniae*,[6] and equinatoxin II from beadlet anemone (*Actinia equine*)[7] all bind a specific lipid and form a pore in the membrane. From a structural point of view, PFTs can be classified as α-PFTs and β-PFTs; the pores of α-PFTs and β-PFTs are composed of α-helices and a β-barrel, respectively.[4] The pore forming activity of PFTs has been investigated by analysis of their induced hemolysis of red blood cells (RBCs) and by leakage of a fluorescent probe from small liposomes such as large unilamellar vesicles (LUVs) using the LUV suspension method.[4,5,7−12] These PFTs are considered to form an oligomer in biomembranes, which then forms a pore. However, the detailed elementary processes and the mechanism of toxin-induced pore formation, including the relationship between oligomers and pores, and characteristics of pores such as membrane permeability remain unclear.

Lysenin is a 33.4 kDa PFT secreted by earthworms (*Eisenia fetida*), which specifically binds sphingomyelin (SM).[8−10] Several experimental data indicate that lysenin molecules form oligomers in lipid membranes that contain SM. Transmission electron microscope images obtained using negative staining show that lysenin molecules form a hexagonal pattern in SM-containing membranes. The unit structure of this hexagon has a diameter of 10−12 nm, which corresponds to that of a lysenin oligomer.[9] It is well established that the lysenin oligomers can be detected using sodium dodecyl sulfate−polyacrylamide gel electrophoresis (SDS−PAGE) because they are resistant to SDS solubilization.[11] Lysenin can induce hemolysis of RBCs.[8] However, preincubation of lysenin with SM-containing liposomes inhibits this hemolysis,[11] and the presence of cholesterol in the SM-containing liposomes increases the efficiency of the inhibition of lysenin-induced

Received: April 8, 2012
Revised: June 5, 2012
Published: June 5, 2012

hemolysis. A recent study showed that an increase in the amount of the SDS-resistant oligomer of lysenin in SM-containing liposomes increased the extent of inhibition of hemolysis described above and also that lysenin monomers in lipid membranes can detach from the membrane and transfer to the RBC membrane, resulting in their hemolysis.[11] These results show that the SDS-resistant oligomer of lysenin cannot either detach from the membrane or dissociate into monomers, indicating that the formation of an SDS-resistant oligomer is an irreversible process. Lipid domains containing SM molecules in plasma membranes or lipid membranes are considered sites of lysenin oligomerization.[12]

Giant unilamellar vesicles (GUVs) of lipid membranes with diameters of >10 μm have been used for investigations of the physical and biological properties of vesicle membranes such as elasticity and shape change.[13−19] Shape changes of a single GUV induced by substances such as peptides, proteins, and small molecules can be measured in real time.[14−19] On the basis of the characteristics of these GUVs, we have recently developed the single-GUV method to investigate the functions and dynamics of biomembranes.[20−27] Using this method, changes in the structure and physical properties of a single GUV that are induced by interactions with substances such as peptides are observed as a function of time and spatial coordinates. The same experiments are then conducted using many "single GUVs", and their results, such as the changes in the physical properties of a single GUV, are statistically analyzed over many single GUVs. This single-GUV method can reveal the details of elementary processes of individual events and allow calculation of their kinetic constants. For example, we explain the single-GUV method studies of pore formation induced by the antimicrobial peptide, magainin 2, in lipid membranes. Using the technique of purification of GUVs containing water-soluble fluorescent probes,[28] we developed the single-GUV method to measure the leakage (or membrane permeation) of internal contents such as fluorescent probes using fluorescence microscopy.[20,25] Then we applied this method to investigate magainin 2-induced leakage and successfully obtained the rate constants of magainin 2-induced pore formation in lipid membranes and also the rate constants of membrane permeation of fluorescent probes through the pores.[25−27] These data provide information that is critical for elucidation of the mechanism of magainin 2-induced pore formation. There are several advantages of the single-GUV method over the LUV suspension method and hemolysis. First, it is easy to identify the cause of the substance-induced membrane permeation (or leakage) of fluorescent probes inside a vesicle. Generally, there are many factors inducing leakage of internal contents of liposomes such as fluorescent probes and leakage of hemoglobin from RBC (i.e., hemolysis), which cannot be identified using the LUV suspension method or hemolysis.[13] For example, membrane fusion by virus induces hemolysis,[29] and polyethylene glycol-induced membrane fusion induces leakage of internal contents of liposomes.[30] Rupture and fragmentation of liposomes or RBCs are also factors of leakage and hemolysis. Factors such as membrane fusion and rupture can be easily detected using the single-GUV method.[21,22] Thereby, the detection of leakage using the LUV suspension method and hemolysis does not always indicate pore formation in lipid membranes. Second, only the use of the single-GUV method allows us to separate the step of substance-induced pore formation in membranes from the step of membrane permeation of a fluorescent probe through the pores and to obtain the rate constants of these elementary steps. Analysis of the latter step can provide values of the membrane permeability coefficient of the fluorescent probe, from which we can gain information about the number of the pores if the membrane permeability coefficient of a single pore does not change over time. To elucidate the effects of mutation of proteins and peptides on the membrane permeation and the effects of lipid compositions or physical properties of lipid membranes on the membrane permeation, we need experimental data that reveal the effects on both the kinetic constant of pore formation and that of membrane permeation through the pore.

The pore forming activity of lysenin has been investigated by analysis of their induced hemolysis of RBCs and by leakage of a fluorescent probe using the LUV suspension method,[8−12] which do not always indicate pore formation, as described in the previous section. In this report, to reveal the interaction of lysenin with SM-containing lipid membranes, we investigated lysenin-induced membrane permeation of fluorescent probes through dioleoylphosphatidylcholine (DOPC)/SM, DOPC/SM/cholesterol (chol), and SM/chol membranes using the single-GUV method. We obtained detailed characteristics of lysenin-induced pore formation and the subsequent membrane permeation of a probe through the pore. We also investigated the effects of lysenin concentration and the presence of cholesterol on lysenin-induced pore formation and membrane permeability. On the basis of the results, we discuss the relationship between the oligomerization of lysenin and lysenin-induced membrane permeability, and also the elementary processes of pore formation.

MATERIALS AND METHODS

Materials. DOPC, SM from brain, 1,2-dipalmitoyl-*sn*-glycero-3-phosphoethanolamine-*N*-[methoxy(polyethylene glycol)-2000] (PEG-2K-DPPE), and 1,2-dioleoyl-*sn*-glycero-3-phosphoethanolamine-*N*-(7-nitro-2-1,3-benzoxadiazol-4-yl) (NBD-DOPE) were purchased from Avanti Polar Lipids Inc. (Alabaster, AL). The Alexa Fluor 488 conjugate of the soybean trypsin inhibitor (AF-SBTI) was purchased from Invitrogen Inc. (Carlsbad, CA). Calcein was purchased from Dojindo Laboratory (Kumamoto, Japan). Bovine serum albumin (BSA) and cholesterol (chol) were purchased from Wako Pure Chemical Industry Ltd. (Osaka, Japan). Lysenin was purchased from the Peptide Institute (Osaka, Japan).

Detection of Lysenin-Induced Membrane Permeation of Fluorescent Probes from Single GUVs. GUVs composed of lipid membranes containing SM were prepared in PBS (1.5 mM KH_2PO_4, 8.1 mM Na_2HPO_4, 137 mM NaCl, and 2.7 mM KCl) by natural swelling of a dry lipid film at 60 °C using the PEG-lipid method.[21,31] In this method, the addition of a small amount of PEG-lipid in lipid membranes allow the preparation of GUVs of electrically neutral lipids such as DOPC and SM in a buffer containing a high salt concentration.[31] Here we used PEG-2K-DPPE as the PEG-lipid and included 1 mol % PEG-2K-DPPE in all the GUV membranes. Two hundred microliters of a 1 mM phospholipid (e.g., SM, DOPC, chol, and 1 mol % PEG-2K-DPPE) mixture in chloroform was placed in a glass vial (5 mL) and dried under a stream of N_2 gas to produce a thin, homogeneous lipid film. The solvent was completely removed by placing the bottle containing the dry lipid film in a vacuum desiccator connected to a rotary vacuum pump for more than 12 h. Next, 20 μL of water was added to this glass vial, and the mixture was

dx.doi.org/10.1021/bi300448g | *Biochemistry* 2012, 51, 5160−5172

incubated at 60 °C for 10 min (prehydration). The hydrated lipid film was then incubated with 1 mL of 1 mM calcein (or 8 μM AF-SBTI) in PBS containing 0.1 M sucrose for 2−3 h at 60 °C. To obtain a purified GUV suspension, untrapped calcein was removed using the membrane filtering method.[32] The GUV suspension was centrifuged at 14000*g* for 20 min at 20 °C to remove multilamellar vesicles. The supernatant was filtered through a nucleopore membrane with 12 μm diameter pores in PBS containing 0.1 M glucose for 1 h at a flow rate of 1 mL/min at room temperature (20−25 °C), and the suspension that was not passed through the filter was collected and used for the following experiments as a purified GUV suspension.

The purified GUV suspension (300 μL) (0.1 M sucrose in PBS as the internal solution; 0.1 M glucose in PBS as the external solution) was transferred into a handmade microchamber.[20,23] A slide glass was coated with 0.1% (w/v) BSA in PBS containing 0.1 M glucose. The GUVs were observed using an inverted fluorescence phase-contrast microscope (IX-70, Olympus, Tokyo, Japan) at 37 ± 1 °C using a stage thermocontrol system (Thermoplate, Tokai Hit, Shizuoka, Japan). Phase-contrast and fluorescence GUV images were recorded using a high-sensitivity EM-CCD camera (C9100-12, Hamamatsu Photonics K.K., Hamamatsu, Japan) with a hard disk. Three neutral density filters (two ND6 and one ND12) were used to decrease greatly the intensity of the incident light to decrease the level of photobleaching of calcein. We did not observe any photobleaching of calcein for at least 10 min under the experimental conditions. The fluorescence intensity inside the GUVs was determined using the AquaCosmos (Hamamatsu Photonics K.K.), and the average intensity per GUV was estimated. Various concentrations of lysenin in PBS containing 0.1 M glucose were continuously added in the vicinity of a GUV through a 20 μm diameter glass micropipet positioned by a micromanipulator. The distance between the GUV and the tip of the micropipet was approximately 70 μm. We consider that this method of application results in the equilibrium lysenin concentration near the GUV being almost the same as that in the micropipet.[20,23] The details of this method are described in our previous reports.[20,26]

Detection of the SDS-Resistant Oligomers of Lysenin by SDS−PAGE. Small unilamellar vesicles (SUVs) of various lipid membranes were prepared using the standard method.[33] PBS was added to the dry lipid film prepared by the same method as described in the preceding section, and the suspension was then sonicated at 55 °C under a N_2-saturated atmosphere using a probe-type ultrasonicator (XL-2000, MISONIX Inc.) and subsequently centrifuged to collect the supernatant. A lysenin solution (187 nM) was incubated with various concentrations of SUVs for various periods of time at 37 °C. Immediately after the incubation, the samples were solubilized in a 2% (w/v) SDS solution containing 2-mercaptoethanol for 5 min at 95 °C and then applied to a 12% gel. The proteins were detected by silver staining using the SilverQuest silver staining kit (Invitrogen Inc.). NIH ImageJ (version 1.45s)[34] was used to obtain the area of the peak corresponding to the monomer or oligomer of lysenin in the gels, and the fraction of lysenin that was present as an SDS-resistant oligomer [(the area of the oligomer peak)/(the area of the oligomer peak and the area of the monomer peak)] was calculated. Lipid concentrations in the SUV suspensions were determined by the Bartlett method.

Detection of Phase Separation Using Confocal Microscopy. To detect phase separation between liquid-ordered and liquid-disordered phases, GUVs of DOPC/SM membranes and DOPC/SM/chol membranes containing 1.0 mol % NBD-DOPE after purification using the membrane filtering method were observed using a confocal microscope (FV-1000, Olympus) at 37 ± 1 °C using a stage thermocontrol system (Thermoplate, Tokai Hit).

RESULTS

Lysenin-Induced Membrane Permeation of Fluorescent Probes in Single SM/DOPC/chol (42/30/28) GUVs. We first investigated lysenin-induced membrane permeation of the fluorescent probe, calcein (Stokes−Einstein radius, R_{SE}, of 0.74 nm),[35] from single SM/DOPC/chol (42/30/28) GUVs. The interaction of lysenin with single GUVs containing 1 mM calcein was conducted in PBS containing 0.1 M glucose at 37 °C and was analyzed by fluorescence microscopy using the single-GUV method. A typical experimental result of the effect of the interaction of 40 ng/mL lysenin with single GUVs on the calcein concentration within a GUV is shown in Figure 1A. Prior to lysenin addition, the GUV displayed high contrast in a phase-contrast microscopic image [Figure 1A(1)] because of

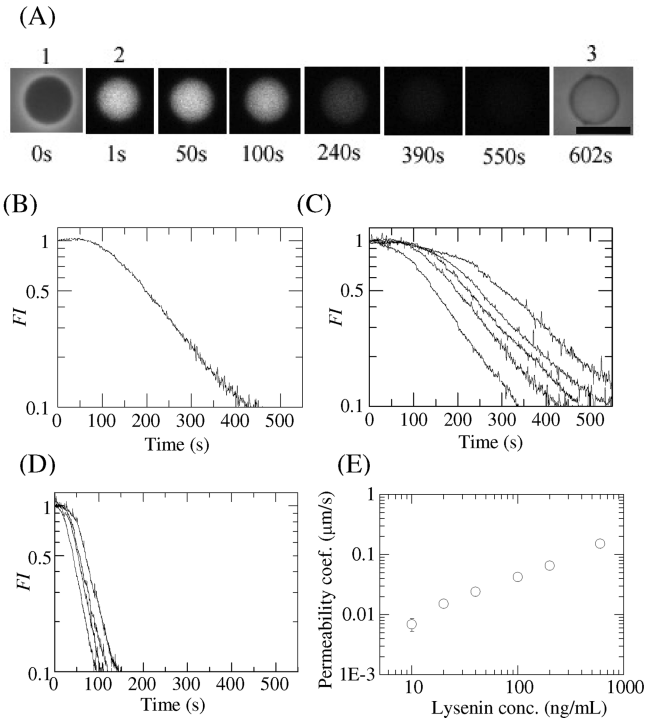

Figure 1. Membrane permeation of calcein from single SM/DOPC/chol (42/30/28) GUVs induced by lysenin at 37 °C. (A) Fluorescence images (2) show that the calcein concentration inside the GUV progressively decreased during the addition of 40 ng/mL lysenin. The numbers below each image show the time in seconds after lysenin addition was started. Also shown are phase-contrast images of the GUV at 0 s (1) and 602 s (3). The bar corresponds to 20 μm. (B) Time course of the change in FI of the inside of the GUV shown in panel A. (C) Other examples of the time course of the change in FI of single GUVs during the addition of 40 ng/mL lysenin. Each curve corresponds to a single GUV. (D) Time course of the change in FI of single GUVs following addition of 200 ng/mL lysenin. Each curve corresponds to a single GUV. (E) Dependence of the membrane permeability coefficient [P^s (μm/s)] at the steady, maximal rate of membrane permeation on lysenin concentration [C (ng/mL)]. The bars indicate standard errors.

dx.doi.org/10.1021/bi300448g | *Biochemistry* 2012, 51, 5160−5172

Table 1. Membrane Permeability Coefficients at the Steady State of the Lysenin-Induced Membrane Permeation of Calcein in Various Membranes at 37 °C[a]

	membrane permeability coefficient at the steady state, P^s (μm/s)		
[lysenin] (ng/mL)	SM/DOPC/chol (42/30/28)	SM/DOPC (58/42)	SM/chol (60/40)
600	$(1.5 \pm 0.2) \times 10^{-1}$ (n = 19)	$(1.8 \pm 0.1) \times 10^{-1}$ (n = 19)	$(2.9 \pm 0.2) \times 10^{-2}$ (n = 20)
200	$(6.5 \pm 0.7) \times 10^{-2}$ (n = 18)	$(3.0 \pm 0.3) \times 10^{-2}$ (n = 19)	$(1.7 \pm 0.2) \times 10^{-2}$ (n = 18)
100	$(4.2 \pm 0.4) \times 10^{-2}$ (n = 16)	$(1.7 \pm 0.1) \times 10^{-2}$ (n = 17)	$(1.0 \pm 0.1) \times 10^{-2}$ (n = 19)
40	$(2.4 \pm 0.2) \times 10^{-2}$ (n = 14)	$(3.0 \pm 0.3) \times 10^{-3}$ (n = 8)	$(1.0 \pm 0.1) \times 10^{-2}$ (n = 15)
20	$(1.5 \pm 0.2) \times 10^{-2}$ (n = 13)	0	$(7.5 \pm 1.6) \times 10^{-3}$ (n = 9)
10	$(6.9 \pm 1.7) \times 10^{-3}$ (n = 8)	0	0
2	0	0	0
0	0	0	0

[a]The average values and the standard errors of membrane permeability coefficients were determined from independent experiments (n is the number of the examined single GUVs).

the difference in the refractive index produced by the difference in the concentration of sucrose and glucose between the inside (0.1 M sucrose) and the outside (0.1 M glucose) of the GUV. A fluorescence microscopic image of the same GUV [Figure 1A(2)] showed a high concentration of calcein inside the GUV at this time. During the addition of the lysenin solution, the fluorescence intensity inside the GUV remained almost constant over the first 50 s, after which the fluorescence intensity decreased gradually [Figure 1A(2)]. Figure 1B shows a semilog plot (base 10) of normalized fluorescence intensity, FI [$=I(t)/I(0)$], versus time (s), where $I(t)$ and $I(0)$ are the fluorescence intensities of the inside of the GUV at time t and that of the intact GUV before initiation of membrane permeation of calcein, respectively. The rate of the decrease in fluorescence intensity (i.e., the absolute value of the slope of the curve) first increased over time and then remained constant after reaching a maximum at 170 s. This maximal rate did not change for up to 450 s. After 450 s, the fluorescence intensity inside the GUV [$I(t)$] had decreased to less than 10% of $I(0)$, although a phase-contrast image of the same GUV [Figure 1A(3)] showed that the GUV structure was still intact with no detectable breaks. During the leakage, large structural changes in GUVs such as association, membrane fusion of GUVs, and large shape changes were not observed. As discussed in our previous report on the interaction of magainin 2 with single GUVs,[25−27] the decrease in fluorescence intensity occurred as a result of the membrane permeation of calcein (i.e., calcein leakage) from the inside to the outside of the GUV through lysenin-induced pores in the membrane. Thus, the time at which the fluorescence intensity began to decrease corresponds to the time at which the first pore was formed in the membrane. Furthermore, a comparison of the phase-contrast images in panels A(1) and A(3) of Figure 1 also showed that there was a substantial decrease in the phase contrast of the GUV, indicating that, during the membrane permeation of calcein, sucrose and glucose also passed through the same pores. When the same experiments were conducted using many single GUVs, we observed that membrane permeation of calcein from a GUV started stochastically, and that the time courses of the changes in the fluorescence intensity of single GUVs were almost the same; i.e., the rate of the decrease in fluorescence intensity first increased over time and then reached a maximum (Figure 1C). This result indicates that pores were formed stochastically, and that the rate of membrane permeation at first increased with time but ultimately reached a maximum.

The rate constant of membrane permeation of the fluorescent probe from the inside to the outside of a GUV, k_{mp}, when membrane permeation starts at time zero, is determined by the following experimental formula:

$$C^{in}(t) = C_0^{in} \exp[-k_{mp}(t)\cdot t] \quad (1)$$

where $C^{in}(t)$ (mol/m^3) and C_0^{in} (mol/m^3) are the concentrations of the fluorescent probe inside of a GUV at time t after and at t_0 before initiation of membrane permeation by lysenin addition, respectively. The normalized concentration of the fluorescent probe inside a GUV, $C^{in}(t)/C_0^{in}$, can be experimentally determined, because the probe concentration inside the GUV is roughly proportional to the fluorescence intensity of the GUV, $I(t)$; i.e., $C^{in}(t)/C_0^{in} = I(t)/I(0) =$ FI. The rate constant of membrane permeation, $k_{mp}(t)$, is proportional to the absolute value of the slope of the curve in a semilog plot (base 10) of FI versus time (s). The results in Figure 1B indicate that k_{mp} at first increased over time and reached a maximum, k_{mp}^s. Moreover, the membrane permeability coefficient of the fluorescent probe per unit area of a GUV membrane, $P(t)$ (m/s), is related to the rate constant of the membrane permeation of the probe, $k_{mp}(t)$, as described in our previous reports.[25,27] Generally, the membrane permeation of a substance can be expressed by the flux of the substance per unit area of pores, J (mol/m^2·s), which follows Fick's law:

$$J = -P(t)[C^{in}(t) - C^{out}(t)] \quad (2)$$

where $C^{out}(t)$ (mol/m^3) is the concentration of the substance outside of the GUV at time t. Thereby, the concentration inside the GUV can be described by $P(t)$ as follows (here we assume $C^{out} = 0$ for any time, because the volume of the outside the GUV is very large):

$$\frac{4\pi r^3}{3}\frac{dC^{in}}{dt} = -4\pi r^2 P(t) C^{in}$$

$$\therefore \frac{d}{dt}\left[\ln \frac{C^{in}(t)}{C_0^{in}}\right] = -\frac{3P(t)}{r} \quad (3)$$

where r (m) is the radius of each GUV. The comparison between eqs 1 and 3 gives

$$P(t) = rk_{mp}(t)/3 \quad (4A)$$

At the steady state of the membrane permeation, $P(t)$ becomes constant ($=P^s$), and thereby, the rate of membrane

dx.doi.org/10.1021/bi300448g | Biochemistry 2012, 51, 5160−5172

permeation of the fluorescent probe from a GUV at the steady state, k^s_{mp}, can be related to P^s as follows:

$$P^s = rk^s_{mp}/3 \quad (4B)$$

The results depicted in Figure 1B indicate that, after pore formation, the value of P increased with time and then reached a steady, maximal value of P^s, which continued for a long time (280 s). To obtain k^s_{mp} values from Figure 1, we fit the region of the curve corresponding to the steady state of the membrane permeation to the following equation.

$$\mathrm{FI}(t) = B \exp[-k^s_{mp}(t - t_a)] \quad (5)$$

where B and t_a are fitting parameters. Using the value of k^s_{mp} and that of the radius of the GUV used in this experiment, the P^s value for Figure 1B was obtained ($P^s = 2.0 \times 10^{-2}$ μm/s). We performed the same experiments using many single GUVs and obtained an average P^s value of $(2.4 \pm 0.2) \times 10^{-2}$ μm/s (the number of the examined single GUVs, n, is 14; i.e., $n = 14$).

We then investigated the interaction of various concentrations of lysenin with single SM/DOPC/chol (42/30/28) GUVs containing 1 mM calcein to obtain the dependence of P^s values on lysenin concentration. The time courses of the changes in FI of many single GUVs during their interaction with 200 ng/mL lysenin are shown in Figure 1D. The absolute values of the slopes of the steady state of membrane permeation of all the curves in Figure 1D were larger than those for 40 ng/mL lysenin. The average value of P^s was $(6.5 \pm 0.7) \times 10^{-2}$ μm/s ($n = 18$). A decrease in the fluorescence intensity of a GUV was not observed at ≤2 ng/mL lysenin. The dependence of P^s on lysenin concentration, C (Figure 1E and Table 1), shows that P^s increased with C. The average value of P^s when 600 ng/mL lysenin was added $[(1.5 \pm 0.2) \times 10^{-1}$ μm/s] was approximately 20 times larger than that of the P^s value for 10 ng/mL lysenin $[(6.9 \pm 1.7) \times 10^{-3}$ μm/s].

To estimate the size of the lysenin-induced pores, we investigated the interaction of lysenin with single SM/DOPC/chol (42/30/28) GUVs containing AF-SBTI (R_{SE} = 2.8 nm).[36] The interaction of 600 ng/mL lysenin with single SM/DOPC/chol (42/30/28) GUVs did not induce a change in the fluorescence intensity of the inside of the GUV, which reflects the concentration of AF-SBTI inside the GUV, over 10 min ($n = 15$) (Figure S1 of the Supporting Information). This result indicates that membrane permeation of AF-SBTI through lysenin-induced pores did not occur. On the basis of these results, we conclude that the radius of the lysenin-induced pore is smaller than 2.8 nm (the R_{SE} of SBTI) but larger than 0.74 nm (the R_{SE} of calcein). This value agrees with the size of the lysenin-induced pores in sheep RBC, which were estimated to have radii of approximately 1.5 nm by assay of inhibition of lysenin-induced hemolysis by various sized substances.[9]

Lysenin-Induced Membrane Permeation of Calcein in Single SM/DOPC (58/42) GUVs. To elucidate the effect of cholesterol on lysenin-induced membrane permeation, we investigated the interaction of lysenin with single SM/DOPC (58/42) GUVs containing 1 mM calcein. The ratio of SM to DOPC in SM/DOPC (58/42) GUVs is the same as that in SM/DOPC/chol (42/30/28) GUVs. Figure 2A shows a typical experimental result of the effect of the interaction of 200 ng/mL lysenin with single GUVs on the calcein concentration within a GUV. As shown in Figure 2A, the lysenin-induced change in the fluorescence intensity of single SM/DOPC (58/42) GUVs was similar to those in SM/DOPC/chol (42/30/28)

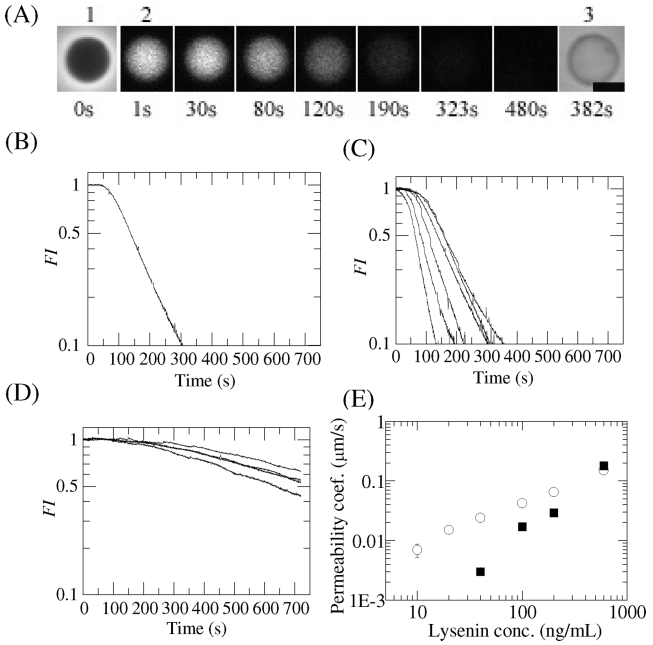

Figure 2. Membrane permeation of calcein from single SM/DOPC (58/42) GUVs induced by lysenin at 37 °C. (A) Fluorescence images (2) show that the calcein concentration inside the GUV progressively decreased during the addition of 200 ng/mL lysenin. The numbers below each image show the time in seconds after the lysenin addition was started. Also shown are phase-contrast images of the GUV at 0 s (1) and 382 s (3). The bar corresponds to 10 μm. (B) Time course of the change in FI of the inside of the GUV shown in panel A. (C) Other examples of the time course of the change in FI of several single GUVs during the addition of 200 ng/mL lysenin. Each curve corresponds to that of each GUV. (D) Time course of the change in FI of the inside of single GUVs during the addition of 40 ng/mL lysenin. Each curve corresponds to that of each GUV. (E) Dependence of P^s (μm/s) on lysenin concentration [C (ng/mL)]. The relationship between P^s and C was plotted for SM/DOPC (58/42) GUVs (■). The bars indicate standard errors. For comparison, the same relationship was also plotted for the SM/DOPC/chol (42/30/28) GUVs (○) that are shown in Figure 1E.

GUVs. During the addition of the 200 ng/mL solution of lysenin, the fluorescence intensity inside the GUV was almost constant over the first 50 s, after which the fluorescence intensity started to decrease gradually (Figure 2B). The rate of the decrease in fluorescence intensity first increased with time but ultimately reached a maximum at 100 s and remained at this level for a long time. We conducted the same experiments using many single GUVs and obtained values of P^s for each GUV (Figure 2C). The average value of P^s was $(3.0 \pm 0.3) \times 10^{-2}$ μm/s ($n = 19$).

We investigated the interaction of various concentrations of lysenin with single SM/DOPC (58/42) GUVs containing 1 mM calcein to obtain the dependence of P^s values on lysenin concentration. For example, Figure 2D shows the time course of FI of many single GUVs during the interaction of 40 ng/mL lysenin. The absolute values of the slopes of the steady sate of membrane permeation of all the curves in Figure 2D were much smaller than those for 200 ng/mL lysenin. The average value of P^s was $(3.0 \pm 0.3) \times 10^{-3}$ μm/s ($n = 8$). Even at 700 s, $I(t)$ values were almost 50% of $I(0)$ ones, but a phase-contrast image of the same GUV showed that the sucrose had completely leaked out and that the GUV structure was still intact with no detectable breaks. This result indicates that the

dx.doi.org/10.1021/bi300448g | Biochemistry 2012, 51, 5160−5172

rate of membrane permeation of sucrose through the pore in these GUVs is much larger than that of calcein. No decrease in the fluorescence intensity of a GUV was observed at lysenin concentrations of ≤20 ng/mL. The dependence of P^s in single SM/DOPC (58/42) GUVs on lysenin concentration, C [Figure 2E (■)], shows that P^s values greatly increased as the lysenin concentration was increased; i.e., P^s values increased as the SM/lysenin ratio decreased, because the SM concentration was the same for all GUVs. The lysenin concentration dependence of P^s of the membranes without cholesterol [SM/DOPC (58/42) GUVs] was much greater than that of P^s of the membranes with cholesterol [SM/DOPC/chol (42/30/28)]. Thus, at low concentrations of lysenin, the P^s values of membranes containing cholesterol [SM/DOPC/chol (42/30/28)] were much larger than those of membranes without cholesterol [SM/DOPC (58/42) GUVs], but at high lysenin concentrations, these P^s values were similar.

Formation of SDS-Resistant Oligomers of Lysenin in Lipid Membranes Containing SM. Several experimental data indicate that lysenin molecules form oligomers in lipid membranes containing SM.[9,11] It is well-established that these oligomers can be detected using SDS−PAGE because they are resistant to SDS solubilization.[5,9,11] The result of SDS−PAGE analysis of a lysenin solution after incubation with SM/DOPC (58/42) SUVs or SM/DOPC/chol (42/30/28) SUVs is shown in Figure 3. The apparent molecular mass of lysenin in PBS is 41 kDa as determined by SDS−PAGE (lane 1 in Figure 3A). After incubation with SM/DOPC (58/42) SUVs for 5 min at 37 °C, a new band with a molecular mass of >260 kDa corresponding to the SDS-resistant oligomer appeared on the gel. The molecular mass of this band is the same as that previously reported.[11] The fraction of lysenin that was present as an SDS-resistant oligomer (i.e., the SDS-resistant oligomer fractions of lysenin) increased as the SM/lysenin molar ratio decreased, and its dependence on the SM/lysenin ratio was much greater in the absence of cholesterol [SM/DOPC (58/42)] than in the presence of cholesterol [SM/DOPC/chol (42/30/28)] (Figure 3B). Thus, at high SM/lysenin ratios, the SDS-resistant oligomer fractions of lysenin in SM/DOPC (58/42) membranes were much lower than that in SM/DOPC/chol (42/30/28) membranes; i.e., the presence of cholesterol increases the fraction of SDS-resistant oligomers, but at low SM/lysenin ratios, these values are similar. These results qualitatively agree with previous results obtained using membranes with different lipid compositions: SM/DOPC (1/4) and SM/DOPC/chol (1/4/1.5).[11] The SDS-resistant oligomer fraction of lysenin in the samples incubated at 37 °C for 2 min was similar to that in samples incubated for 30 min (Figure 3C). This result indicates that the rate at which SDS-resistant oligomers of lysenin form in the lipid membrane is very fast and that most of the oligomerization processes occur within the first 2 min of incubation at 37 °C.

Phase Separation of SM/DOPC/chol GUVs and SM/DOPC GUVs. It is well-known that the phase separation between the liquid-ordered (lo) phase domain and the liquid-disordered (ld) phase domain occurred in SM/DOPC/chol membranes.[37] To check the phase separation, a small amount (1 mol % in the total membrane lipids) of a fluorescence probe, NBD-DOPE, was included in the SM/DOPC/chol GUVs and SM/DOPC GUVs. Figure 4A shows confocal fluorescence microscopic images of a SM/DOPC/chol (42/30/28) GUV in PBS. Clear large phase separation was observed, and the domains with high fluorescence intensities correspond to the ld

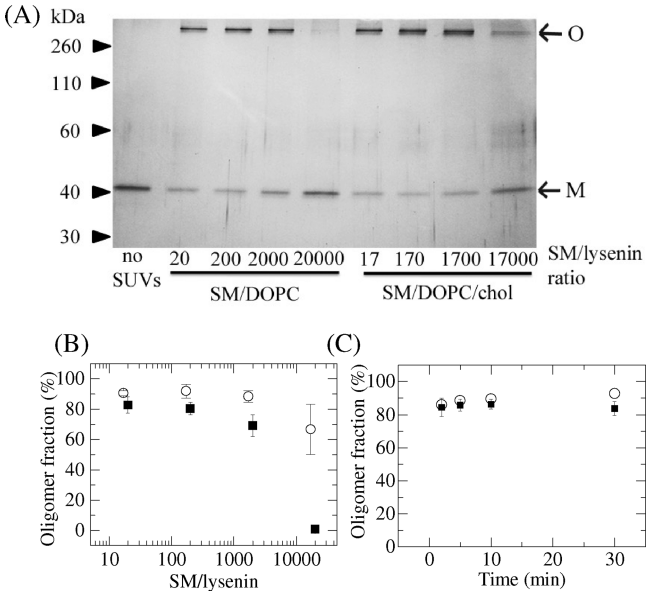

Figure 3. SDS-resistant oligomerization of lysenin in the presence of lipid membranes containing SM. (A) A lysenin solution (187 nM) was incubated with SM/DOPC (58/42) SUVs or SM/DOPC/chol (42/30/28) SUVs at various SM/lysenin molar ratios (20−20000 or 17−17000, respectively) for 5 min at 37 °C. The samples were then analyzed by SDS−PAGE (silver staining). The lysenin monomer and oligomer are indicated by M and O, respectively. (B) Quantification of the dependence of the SDS-resistant oligomer fraction on the SM/lysenin molar ratio shown in panel A: SM/DOPC/chol (42/30/28) SUVs (○) and SM/DOPC (58/42) SUVs (■). (C) Quantification of the dependence of the SDS-resistant oligomer fraction on incubation time with SM/DOPC/chol (42/30/28) SUVs (○) and SM/DOPC (58/42) SUVs (■). SM/lysenin molar ratios for SM/DOPC/chol (42/30/28) SUVs and SM/DOPC (58/42) SUVs were 4000 and 2500, respectively. For panels B and C, the SDS-resistant oligomer fraction was calculated as the percent of total lysenin that is present as an oligomer [oligomer fraction (%)], and the average values of the oligomer fraction were obtained from two independent experiments. The bars indicate standard errors.

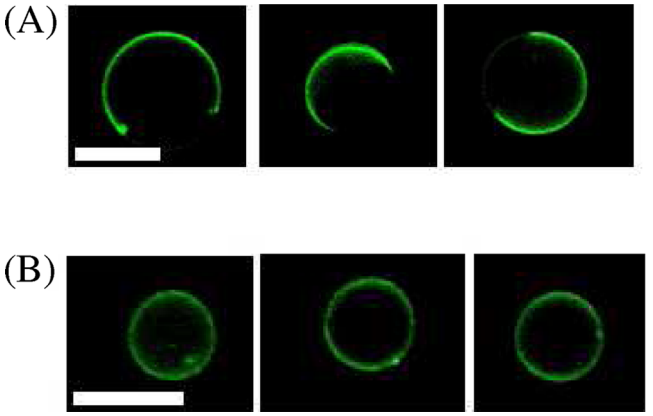

Figure 4. Phase separation of lipid membranes between lo and ld phases in SM/DOPC/chol (42/30/28) GUVs (A) and SM/DOPC (58/42) GUVs (B). The domains with high fluorescence intensities correspond to the ld phase. The bars correspond to 20 μm.

phase.[29] The lo phase domains are very large, and the number of domains was small. These results indicate that the fluorescence microscopy system we used here can clearly reveal large phase separation in SM/DOPC/chol (42/30/28)

dx.doi.org/10.1021/bi300448g | Biochemistry 2012, 51, 5160−5172

GUVs. In contrast, the fluorescence microscopic image of a SM/DOPC (58/42) GUV (Figure 4B) shows that the phase separation occurred and there were many small lo phase domains.

Lysenin-Induced Membrane Permeation of Calcein in Single SM/chol (60/40) GUVs. In the interaction of lysenin with SM/DOPC/chol (42/30/28) GUVs, lysenin may preferentially produce pores in SM/chol-rich domains in the lo phase, as demonstrated in the interaction of lysenin with cells.[12] To elucidate lysenin-induced pore formation in the homogeneous lo phase membrane, we next investigated the interaction of lysenin with calcein (1 mM)-containing single GUVs composed of a SM/chol (60/40) membrane that is completely in the lo phase,[23,24] under the same conditions described above. Figure 5A shows a typical experimental result

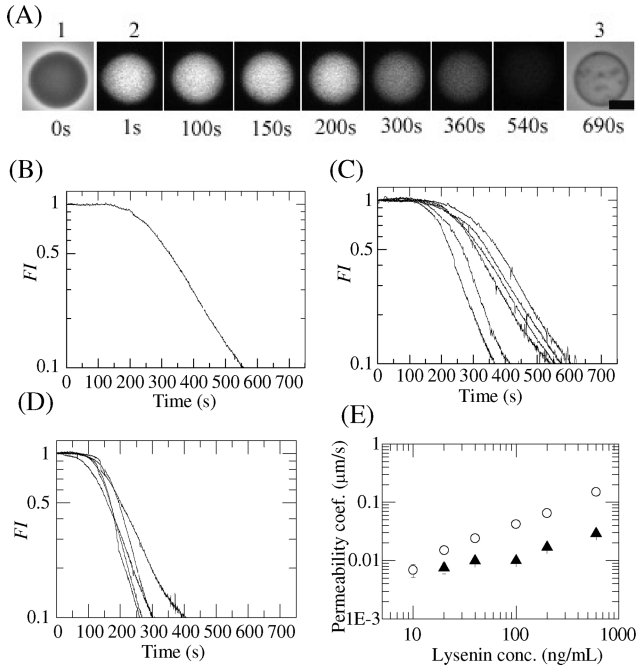

Figure 5. Membrane permeation of calcein from single SM/chol (60/40) GUVs induced by lysenin at 37 °C. (A) Fluorescence images (2) show that the calcein concentration inside the GUV progressively decreased during the addition of 40 ng/mL lysenin. The numbers below each image show the time in seconds after the lysenin addition was started. Also shown are phase-contrast images of the GUV at 0 s (1) and 690 s (3). The bar corresponds to 10 μm. (B) Time course of the change in FI of the inside of the GUV shown in panel A. (C) Other examples of the time course of the change in FI of the inside of single GUVs during the addition of 40 ng/mL lysenin. Each curve corresponds to that of each GUV. (D) Time course of the change in FI of the inside of single GUVs during the addition of 200 ng/mL lysenin. Each curve corresponds to that of each GUV. (E) Dependence of P^s (μm/s) on lysenin concentration [C (ng/mL)]. The relationship between P^s and C is plotted for SM/chol (60/40) GUVs (▲). The bars indicate the standard error. For comparison, the same relationship was also plotted for the SM/DOPC/chol (42/30/28) GUVs (○) that are shown in Figure 1E.

of the effect of the interaction of 40 ng/mL lysenin with single GUVs on the calcein concentration within a GUV. During the addition of the 40 ng/mL solution of lysenin, the fluorescence intensity inside the GUV was almost constant over the first 140 s, after which the fluorescence intensity started to decrease gradually [Figure 5A(2) and Figure 5B]. The rate of the decrease in fluorescence intensity increased with time and then reached a steady maximum at 300 s. After 690 s, no fluorescence could be detected inside the GUV, although a phase-contrast image of the same GUV [Figure 5A(3)] showed that the GUV structure was still intact with no detectable breaks. From the plot of FI versus time, we obtained P^s. In the 40 ng/mL lysenin-induced pore, P^s was relatively large [i.e., $P^s = (1.0 \pm 0.1) \times 10^{-2}$ μm s^{-1}] ($n = 15$). When the same experiments were conducted using many single GUVs, we observed that the membrane permeation of calcein from a GUV started stochastically, but the time courses of the fluorescence intensity of single GUVs were almost the same; i.e., the rate of the decrease in fluorescence intensity increased with time and then reached a steady maximum (Figure 5C).

We then investigated the interaction of various concentrations of lysenin with single SM/chol (60/40) GUVs containing 1 mM calcein to obtain the dependence of P^s values on lysenin concentration. The time courses of the changes in FI of many single GUVs during their interaction with 200 ng/mL lysenin are shown in Figure 5D. The absolute values of the slopes of the steady state of membrane permeation of all the curves in Figure 5D were larger than those for 40 ng/mL lysenin. The average value of P^s was $(1.7 \pm 0.2) \times 10^{-2}$ μm/s ($n = 18$). A decrease in the fluorescence intensity of a GUV was not observed at lysenin concentrations of ≤10 ng/mL. The lysenin concentration (C) dependence of P^s in single SM/chol (60/40) GUVs [Figure 5E (▲) and Table 1] shows that P^s gradually increases with an increase in C. Furthermore, the dependence of P^s on C was much weaker in SM/chol (60/40) GUVs than in SM/DOPC/chol (42/30/28) GUVs, and the P^s values of SM/chol (60/40) GUVs were much smaller than those of SM/DOPC/chol (42/30/28) GUVs at high concentrations of lysenin.

We also investigated the SDS-resistant oligomer formation in SM/chol (60/40) membranes. The result of SDS−PAGE analysis of a lysenin solution after incubation with SM/chol (60/40) SUVs is shown in Figure 6. The SDS-resistant oligomer fractions of lysenin in SM/chol (60/40) membranes gradually increased as the SM/lysenin molar ratio decreased, and its dependence on the SM/lysenin ratio was almost the same as that of SM/DOPC/chol (42/30/28) membranes. The SDS-resistant oligomer fraction of lysenin in the SM/chol (60/40) membranes incubated at 37 °C for 2 min was similar to that in samples incubated for 30 min (Figure 6C). This result indicates that the rate at which SDS-resistant oligomers of lysenin form in the lipid membrane is very fast and that most of the oligomerization processes occur within the first 2 min of incubation at 37 °C.

■ DISCUSSION

Correlation between Lysenin-Induced Membrane Permeation and the SDS-Resistant Oligomer Fraction of Lysenin. The results obtained using the single-GUV method clearly show that lysenin induced pores in three kinds of lipid membranes and the membrane permeation of calcein occurred through the pores without the disruption of the GUVs. It is reported that high concentrations of His-lysenin caused fragmentation of liposomes.[38] If we were to investigate the His-lysenin-induced leakage of a fluorescent probe using the LUV suspension method, we would not be able to distinguish between pore formation and the fragmentation of liposomes. The membrane permeation of calcein began stochastically at the initial stage of the interaction of lysenin with a GUV.

dx.doi.org/10.1021/bi300448g | Biochemistry 2012, 51, 5160−5172

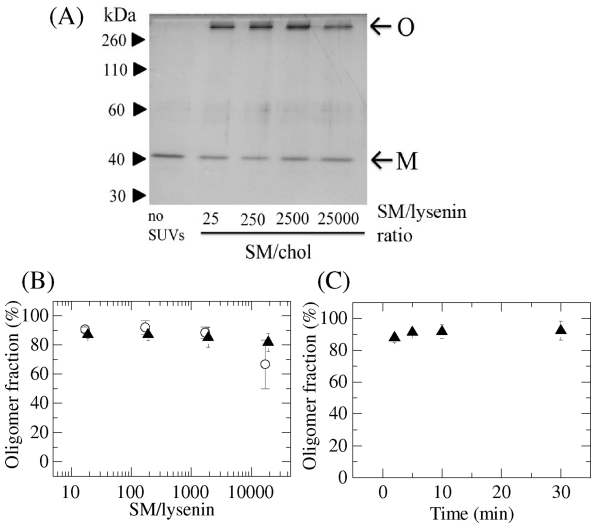

Figure 6. SDS-resistant oligomerization of lysenin in the presence of lipid membranes containing SM. (A) A lysenin solution (187 nM) was incubated with SM/chol (60/40) SUVs at various SM/lysenin molar ratios (25−25000) for 5 min at 37 °C. The samples were then analyzed by SDS−PAGE (silver staining). The lysenin monomer and oligomer are indicated by M and O, respectively. (B) Quantification of the dependence of the SDS-resistant oligomer fraction of lysenin on the SM/lysenin molar ratio shown in panel A: SM/chol (60/40) SUVs (▲) and SM/DOPC/chol (42/30/28) SUVs (○). (C) Quantification of the dependence of the SDS-resistant oligomer fraction of lysenin on incubation time with SM/chol (60/40) SUVs (▲). The SM/lysenin molar ratio was 1900. For panels B and C, the SDS-resistant oligomer fraction was calculated as the percent of total lysenin that is present as an oligomer [oligomer fraction (%)], and the average values of the oligomer fraction were obtained from two independent experiments. The bars indicate standard errors.

Subsequently, the membrane permeability coefficient increased over time to reach a steady maximum, P^s, which persisted for a long time (100−500 s). We succeed in determining P^s values under various conditions. The results showed a strong correlation between the lysenin-induced membrane permeability coefficient and SDS-resistant oligomerization of lysenin in SM/DOPC (58/42) and SM/DOPC/chol (42/30/28) membranes. The SDS-resistant oligomer fraction of lysenin and the P^s values increased as the SM/lysenin ratio decreased, and the lysenin concentration dependence of the SDS-resistant oligomer fractions and that of the P^s values of the membrane without cholesterol [SM/DOPC (58/42) GUVs] were much greater than those of the membrane with cholesterol [SM/DOPC/chol (42/30/28)]. Therefore, at low concentrations of lysenin, the SDS-resistant oligomer fraction and the P^s values of SM/DOPC/chol (42/30/28) membranes were much higher than those of SM/DOPC (58/42) membranes, but these values were similar at high lysenin concentrations.

If we consider that lysenin molecules form a specific oligomer in lipid membranes containing SM and form pores that all have the same diameter, the value of $P(t)$ of the lipid membrane is determined by the permeability coefficient of a single pore, P_1, the fraction of the open state of the pore (i.e., the probability of opening), P_{open},[39] and the pore concentration (i.e., the number of pores per unit area), $N_P(t)$; i.e., $P(t) = P_1P_{open}N_P(t)$. We can therefore interpret the results of Figures 1 and 2 as follows. The data in Figures 1C and 2C indicate that a pore is first formed in the lipid membrane, after which N_P increases over time and finally reaches a steady maximum, N_P^s. The data in Figure 2E suggest that the value of N_P^s increases as the lysenin concentration in the buffer increases and that at low concentrations of lysenin N_P^s values of membranes containing cholesterol [SM/DOPC/chol (42/30/28)] are much larger than those of membranes without cholesterol [SM/DOPC (58/42) GUVs], but at high concentrations of lysenin, these values are similar.

On the basis of the preceding discussion, we can reasonably conclude that N_P^s increases as the SDS-resistant oligomer fraction of lysenin increases in lipid membranes. On the other hand, the P^s of SM/chol (60/40) GUVs was much smaller than that of SM/DOPC/chol (42/30/28) GUVs (Figure 5E), even though the SDS-resistant oligomer fractions of lysenin were similar in both membranes (Figure 6B). These results indicate that not all of the oligomers in the membrane can convert into pores. In both membranes, the concentration of oligomer [correctly speaking, concentration of irreversible oligomer (see the following section)], $N_o(t)$, increased with lysenin concentration in buffer because the SDS-resistant oligomer fractions were similar irrespective of lysenin concentration (Figure 6B), and thereby, Figure 5E indicates that P^s increased with N_o^s, i.e., the N_o value at the steady state. On the basis of the preceding discussion, we can conclude that some portion of the lysenin oligomers can convert into pores, and that the following equation can be held as an approximation of the relationship between N_P^s and N_o^s; $N_P^s = \beta N_o^s$ (where β is a constant that depends on the physical property of the membrane), where the value of β for SM/chol (60/40) membranes is smaller than that for SM/DOPC/chol (42/30/28) membranes. Moreover, we can conclude that the SDS-resistant oligomer fractions of lysenin represent both the oligomers that comprise pores and the irreversible oligomers before conversion to pores, and thereby, these results provide the first experimental evidence that the SDS-resistant oligomer is not equal to the pore.

Lysenin-Induced Pore Formation in Lipid Membranes. In this section, we analyze the lysenin-induced pore formation more quantitatively. After the interaction of lysenin with single GUVs had begun, the fluorescence intensities inside the GUVs were almost constant over the first specific period, after which the fluorescence intensity started to decrease gradually and stochastically, indicating that the formation of the first pore in lipid membranes occurred stochastically. During the initial time when the fluorescence intensities inside the GUVs were almost constant, lysenin in buffer binds to SM molecules in the lipid membrane and lysenin monomers bound with SM form an oligomer, and then a pore is formed. As demonstrated in our previous reports,[25,26] when the rate constant of pore formation is being estimated, the time course of the fraction of intact GUV, $P_{intact}(t)$, from which calcein did not start to leak among the population of GUVs examined is important. When $P_{intact}(t)$ rapidly decreases with time, the rate of pore formation is large. If the rate-determining step of pore formation can be considered as a two-state transition (or conversion), $P_{intact}(t)$ decreases exponentially with time. In the case of magainin 2, we considered the two-state transition model from the binding state to the pore state, and thereby, P_{intact} of GUVs in the presence of various concentrations of magainin 2 can be fit well by a single-exponential decay function defined as follows:[25,26]

$$P_{intact}(t) = \exp[-k_P(t - t_{eq})] \quad (6)$$

dx.doi.org/10.1021/bi300448g | Biochemistry 2012, 51, 5160−5172

where k_P is the rate constant of the two-state transition and t_{eq} is a fitting parameter. However, in other cases, P_{intact} may decrease pseudoexponentially with time.

We can estimate the rate of lysenin-induced pore formation by the time course of $P_{intact}(t)$. Figure 7A shows that P_{intact} of

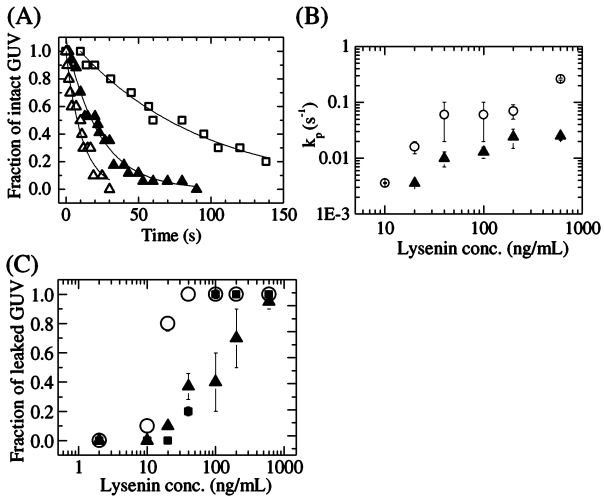

Figure 7. Rates of lysenin-induced pore formation in three kinds of membranes. (A) Time course of P_{intact} of SM/DOPC/chol (42/30/28) GUVs in the presence of (△) 200, (▲) 40, and (□) 20 ng/mL lysenin. The solid lines represent the best-fit curves of eq 6. (B) Dependence of k_P on lysenin concentration in PBS: (○) SM/DOPC/chol (42/30/28) and (▲) SM/chol (60/40) GUVs. We conducted two or three independent experiments for a given lysenin concentration using 10−20 single GUVs in each experiment and obtained average values and standard errors of k_P. (C) Dependence of $P_{LS}(120\ s)$ on lysenin concentration: (○) SM/DOPC/chol (42/30/28), (■) SM/DOPC (58/42), and (▲) SM/chol (60/40) GUVs. The bars indicate the standard error.

SM/DOPC/chol (42/30/28) GUVs decreased with time in the presence of various concentrations of lysenin, which were almost fit by a single-exponential decay function defined by eq 6. The rate constant of pore formation increased with an increase in lysenin concentration: the average k_P of 600 ng/mL lysenin $[(2.6 \pm 0.1) \times 10^{-1}\ s^{-1}]$ was ∼70 times larger than that of k_P for 10 ng/mL lysenin $[(3.6 \pm 0.1) \times 10^{-3}\ s^{-1}]$ (Figure 7B). The k_P values of SM/chol (60/40) GUVs were much smaller than those of SM/DOPC/chol (42/30/28) GUVs, irrespective of lysenin concentration (Figure 7B). In contrast, in the case of SM/DOPC (58/42) GUVs, several curves of the time course of P_{intact} were not fit well by a single-exponential function. However, we can roughly compare the rate of pore formation using the fraction of leaked GUV, $P_{LS}(t)$, i.e., the fraction of GUVs in which leakage had already started, among all the examined GUVs.[21,25] Thus, $P_{LS}(t) = 1 - P_{intact}(t)$. Figure 7C shows $P_{LS}(120\ s)$ for all the examined GUVs. At low concentrations of lysenin, the $P_{LS}(120\ s)$ values of SM/DOPC/chol (42/30/28) membranes were much higher than those of SM/DOPC (58/42) membranes, but these values were similar at high lysenin concentrations. This result suggests that at low concentrations of lysenin, the rates of pore formation of SM/DOPC/chol (42/30/28) membranes were much higher than those of SM/DOPC (58/42) membranes, but these values were similar at high lysenin concentrations.

In general, many kinds of schemes for PFT-induced pore formation have been proposed. For example, PFT molecules in a buffer bind to a lipid membrane; a monomer of the bound PFT can diffuse laterally in the membrane and collide with other monomers to form an oligomer, and then a conformational change induces oligomer to pore conversion.[4,40] In some PFTs, insertion of protein segments may occur in the binding of monomer PFT, but in others, insertion of protein segments occurs in the oligomer to pore conversion. For lysenin-induced pore formation, we can consider several schemes involved in intermediate states (i.e., the oligomer states), but at present, we cannot identify the right scheme because of limited experimental data. Here we consider a few models of lysenin-induced pore formation in lipid membranes containing SM. A lysenin molecule in a buffer surrounding a single GUV can bind to the SM molecules in the lipid membranes specifically, and the binding equilibrium is attained very rapidly.[8] We call this lysenin the monomer lysenin. Several monomer lysenin molecules in the lipid membrane form an oligomer lysenin,[11] which induces a pore in lipid membranes. This lysenin-induced pore formation is composed of two elementary steps: the formation of the lysenin oligomer (i.e., oligomerization step) and oligomer-induced pore formation (i.e., pore formation step). We can consider two cases of the reaction schemes; in case 1, the oligomerization step is rapid and pore formation is the rate-determining step, and in case 2, the oligomerization step is the rate-determining step and immediately after the oligomerization a pore is formed. In case 1, the scheme of the reaction of pore formation can be represented as follows:

$$N(\text{monomer}) \Leftrightarrow (\text{reversible oligomer}) \Rightarrow (\text{irreversible oligomer}) \rightarrow (\text{pore})$$

Here we assume the presence of reversible oligomers that can reversibly convert to the monomer, based on the general tendency of protein association, although we do not have any experimental evidence of the existence of the reversible oligomer lysenin. We can reasonably consider that the lysenin irreversible oligomer that cannot convert to the monomer is the same as the prepore revealed in the case of β-PFTs.[1,40] As described in the preceding section, the SDS-resistant oligomer fractions of lysenin represent both the irreversible oligomers and the pores. In case 1, the conversion of the irreversible oligomer (or prepore) to the pore is slow and the rate-determining step. $N_o(t)$, defined in the previous section, is the concentration of the irreversible oligomer. Pore formation in the SM/chol (60/40) membrane may follow the scheme of case 1, because the results in this report indicate that $N_o(t)$ is large but $N_p(t)$ is small. If the rate of irreversible oligomer formation from the lysenin monomer in lipid membranes is very large and the conversion of irreversible oligomer to pore is very slow, pore formation can be approximated as the two-state transition, and thereby, k_P can be regarded as the rate constant for the conversion from the irreversible oligomer state to the pore state. In other cases, k_P may be obtained by a pseudoexponential decay of P_{intact} of GUVs. On the other hand, in case 2, the scheme of the reaction of pore formation can be represented as follows:

$$N(\text{monomer}) \leftrightarrow (\text{reversible oligomer}) \rightarrow (\text{irreversible oligomer}) \Rightarrow (\text{pore})$$

dx.doi.org/10.1021/bi300448g | Biochemistry 2012, 51, 5160−5172

In general, there are many pathways of monomer oligomerization,[40] and the rate of oligomerization depends on the pathway. In case 2, the rate of pore formation equals that of oligomerization, and thereby, the rate constant k_P determined by the single-exponential decay or the pseudoexponential decay of P_{intact} of SM/DOPC/chol (42/30/28) GUVs (Figure 7A) is that of oligomerization. In other cases, a single-exponential decay or a pseudoexponential decay of P_{intact} of GUVs may be observed. Irrespective of the schemes of lysenin-induced pore formation, the results in panels B and C of Figure 7 indicate that the rate of pore formation increased with lysenin concentration depending on the lipid compositions of the membranes; at low concentrations of lysenin, the values of the rate of pore formation of SM/DOPC/chol (42/30/28) membranes were much higher than those of SM/DOPC (58/42) membranes, but these values were similar at high lysenin concentrations.

We consider that, at equilibrium, a portion of the lysenin monomers (αM_0, where M_0 is lysenin monomer concentration in a lipid membrane before the start of oligomerization) change into the irreversible oligomers (i.e., $N_O = \alpha M_0/N$, where N is the number of monomers that form an oligomer). In the case where the formation of oligomer is irreversible as in cases 1 and 2, eventually almost all the monomers change into the irreversible oligomers (i.e., $\alpha \approx 1$). Subsequently, a part of the irreversible oligomers change (βN_O) into pores; the final pore concentration is $N_P^{eq} = \alpha\beta M_0/N$. As described in the previous section, $P(t) = P_1 P_{open} N_P(t)$, and therefore, the final equilibrium value of $P(t)$, P^{eq}, is proportional to M_0, because $P^{eq} = P_1 P_{open} N_P^{eq} = P_1 P_{open} \alpha\beta M_0/N$. We can reasonably consider that the binding of lysenin with lipid membranes that contain SM molecules follows the Langmuir adsorption isotherm, and therefore, M_0 is determined as follows:

$$M_0 = \frac{AK_BC}{1 + K_BC} = A\left(1 - \frac{1}{1 + K_BC}\right) \quad (7)$$

where C is the lysenin concentration in buffer, K_B is the binding constant of lysenin with SM, and A is the concentration of lysenin binding sites composed of several SM molecules. It should be noted that in single-GUV experiments the lysenin concentration around the GUV is always constant, and that this condition is used to derive eq 7. Therefore, P^{eq} is determined by C and A as follows:

$$P^{eq} = \frac{P_1 P_{open} \alpha\beta}{n} M_0 = \frac{P_1 P_{open} \alpha\beta A}{n}\left(1 - \frac{1}{1 + K_BC}\right) \quad (8)$$

This relationship indicates that the dependence of P^{eq} on lysenin concentration follows the Langmuir isotherm type of equation. If the rate of oligomerization and that of conversion from an oligomer to a pore are rapid, P^s can be approximated as P^{eq}.

The localization of SM molecules in the lipid membranes may play an important role in lysenin-induced pore formation. As shown in Figure 4, phase separation occurs in SM/DOPC/chol and SM/DOPC membranes; SM/chol-rich microdomains appear in SM/DOPC/chol membranes, and SM-rich domains appear in SM/DOPC membranes.[37] Atomic force microscopy also reveals the phase separations in SM/DOPC membranes with similar compositions.[38,41] SM/chol-rich domains are in the lo phase, and therefore, the diffusion coefficients of lipid molecules are relatively high. Thus, lysenin molecules bound to SM molecules in SM/chol-rich domains can rapidly diffuse within this domain and frequently collide with other lysenin molecules bound to SM molecules, resulting in a high rate of lysenin oligomerization and subsequent pore formation. In this situation, we can assume that the experimentally determined value of P^s is almost equal to that of P^{eq}. The dependence of P^s in single SM/DOPC/chol (42/30/28) GUVs on C (nM) (same data as in Figure 1E) fit well to eq 8 [Figure 8A (○)].

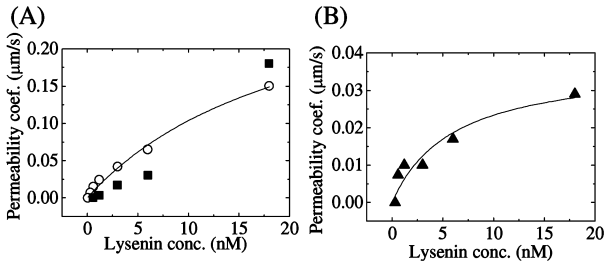

Figure 8. (A) Dependence of P^s (μm/s) on C (nM) for SM/DOPC/chol (42/30/28) GUVs (○) and SM/DOPC (58/42) GUVs (■). Experimental data of SM/DOPC/chol (42/30/28) GUVs were fit well using the Langmuir adsorption isotherm (eq 8). (B) Dependence of P^s (μm/s) on C (nM) for SM/chol (60/40) GUVs (▲). Experimental data were fit well using the Langmuir adsorption isotherm (eq 8).

On the basis of this fitting, a lysenin−SM binding constant (K_B) of 0.046 nM^{-1} was obtained. Similarly, the dependence of P^s in single SM/chol (60/40) GUVs on C (nM) also fit well to eq 8 (Figure 8B) and a lysenin−SM binding constant (K_B) of 0.17 nM^{-1} was obtained. These values of K_B were almost the same as the K_B value for the SM/chol (50/50) membrane (0.12 nM^{-1}).[8] The other information obtained by this fitting was the value of $P_1 P_{open} \alpha\beta A/N$, which was 0.33 μm/s for SM/DOPC/chol (42/30/28) and 0.037 μm/s for SM/chol (60/40) membranes.

It is worth trying to obtain the value of the permeability coefficient of a single pore, P_1. Recent single-channel recording measurement of the lysenin-induced pore showed no observable closing events of the pore, indicating that $P_{open} = 1$.[42] However, lysenin with a polyhistidine tag (lysenin-His) induced channel activity with closing events in other lipid membranes, indicating that $P_{open} < 1$.[38] The difference between these results may be due to the presence of polyhistidine tag or different lipid compositions. Here we approximate that the lysenin-induced pore is always in the open state; i.e., $P_{open} = 1$. If we assume that the oligomer of lysenin that is present in the lipid membranes is a hexamer (i.e., $N = 6$) and that 100% of the monomer changes into pores (i.e., $\alpha = \beta = 1$), then $P_1 A/n = 0.33$ in SM/DOPC/chol (42/30/28) GUVs, and the value of P_1 can be estimated to be 1.7×10^{-5} $\mu m^3/s$.

In contrast, the physical property of the SM-rich domains in SM/DOPC membranes and the behavior of the SM-bound lysenin are not very clear. It is certain that the SM-rich domain contains some fractions of DOPC molecules from the point of view of the physics of phase separation.[43−45] To obtain the accurate SM (or DOPC) concentration in the SM-rich domains after phase separation, we need a phase diagram of temperature versus SM concentration for SM/DOPC membranes,[44] but it is lacking. Moreover, differential scanning calorimetry revealed that a broad gel-to-liquid crystalline (L_α) phase transition with a maximum at 41 °C occurs in the pure SM membrane because of the multicomponent mixture of hydrocarbon chains,[46] indicating that some portions of SM molecules are in the ld

dx.doi.org/10.1021/bi300448g | Biochemistry 2012, 51, 5160−5172

phase under our experimental conditions. At present, we have a hypothesis. The SM-rich domains in SM/DOPC (58/42) GUVs are in the solid-ordered (so) or gel phase, and therefore, the diffusion coefficients of the lipid molecules are low. In this case, the frequency of collision of lysenin molecules due to lateral diffusion is low. However, at high concentrations of the bound lysenin monomer, these SM-bound lysenin molecules are close to each other in the membrane, and therefore, even a small movement or change in orientation can induce their oligomerization. Hence, at low concentrations of lysenin, the P^s values were very small, but at high concentrations of lysenin, the P^s values were very large, which were similar to those of SM/DOPC/chol (42/30/28) GUVs. This may be why the dependence of P^s in single SM/DOPC (58/42) GUVs on lysenin concentration did not fit to eq 8. The SM concentration in the SM-rich domains after phase separation in the SM/DOPC (58/42) membrane is >58 mol %. We observed lysenin-induced membrane permeation of calcein with values of P^s in SM/DOPC (90/10) GUVs similar to those in SM/DOPC (58/42) GUVs [$P^s = (1.7 \pm 0.3) \times 10^{-1}$ μm/s ($n = 5$) for 600 ng/mL lysenin] (Figure S2 of the Supporting Information). The confocal fluorescence microscopic images of SM/DOPC (90/10) GUVs suggest no phase separation occurred at the resolution of the optical microscopic image, although nanoscale phase separation may occur (Figure S2D of the Supporting Information). This SM/DOPC (90/10) membrane may have a composition similar to that of the SM-rich domains in SM/DOPC (58/42) GUVs, although it may have small amounts of the ld phase (i.e., the mixture of so and ld phases). Thereby, this result may suggest that lysenin can form pores in the SM-rich domains.

At present, we do not have experimental evidence to explain the mechanism for the result that the P^s of SM/chol (60/40) GUVs was much smaller than that of SM/DOPC/chol (42/30/28) GUVs even though the SDS-resistant oligomer fractions of lysenin were similar in both membranes. We have a hypothesis about the mechanism. For the formation of a pore, it is necessary that protein segments of lysenin insert into the lipid membrane to form a pore. The insertion of a pore composed of protein segments into lipid membrane increases the lateral pressure. Thereby, further insertion of protein segments is suppressed.[47] Particularly for SM/chol (60/40) membranes, all of the membrane regions have a large area compressibility modulus,[48] and therefore, the rate of insertion of segments is low and the number of the inserted segments or the number of the pores is small because of the high lateral pressure. In contrast, in the case of SM/DOPC/chol (42/30/28) membranes, these membranes contain ld phase regions where the elastic modulus is small,[37] and therefore, a relatively large number of protein segments can enter into the membrane, which increases the number of pores that can be formed.

Biological Implications. The results in this report clearly show that low concentrations of lysenin can rapidly form pores in SM/DOPC/chol GUVs using SM/chol-rich microdomains in the lo phase. Many cells have similar microdomains (or rafts) in plasma membranes that are composed of SM, cholesterol, and several proteins such as GPI-anchored proteins, which are in the lo phase, and they are thought to play important roles in signal transduction.[49] Therefore, these microdomains in plasma membranes are very suitable targets for lysenin, because low concentrations of lysenin can rapidly form many pores in the plasma membrane to induce cytolysis and kill the cells. Sobota and his colleague found that during fractionation of Triton X-100 cell lysates SDS-resistant oligomers of lysenin with a glutathione *S*-transferase (GST) tag associated with membrane fragments that were insoluble in Triton X-100, supporting the above conclusion.[12]

It is considered that the phase boundary between the lo and ld phases plays an important role in pore formation of another PFT, equinatoxin II.[50] However, our results clearly show that lysenin does form a pore in a complete, homogeneous lo phase membrane [i.e., SM/chol (60/40)] (Figure 5), indicating that lysenin-induced pore formation can occur in the absence of the phase boundary. At present, we do not know the structure of the lysenin-induced pore. However, to form a stable pore in a lipid membrane, protein segments such as α-helix or β-sheet must insert into lipid membranes. Thereby, these results indicate that a protein segment can easily insert into a lipid membrane in the pure lo phase to form a pore. This possibility is supported by our previous results that lipids with a single long hydrocarbon chain such as lysophosphatidylcholine can insert into a complete, homogeneous lo phase membrane from an aqueous solution outside of single GUVs.[23,24]

Advantages and an Inherent Problem in This Stage of the Single-GUV Method. Using the single-GUV method, we succeeded in separating one elementary step (i.e., lysenin-induced pore formation) from the other elementary step (i.e., membrane permeation of fluorescent probes through the pores) and in obtaining information about the rate constant or the rate of pore formation and the membrane permeability coefficient of the fluorescent probe and its dependence on time.

However, there is a problem in the current stage of the single-GUV method, i.e., the accuracy of the rate constants of the elementary steps. As shown in Table 1 and Figures 2E and 5E, the standard errors of the membrane permeability coefficients are 10−20% of the average values when 10−20 single GUVs were examined. Thereby, the membrane permeability coefficients have two significant digits. On the other hand, the standard errors of the rate constant of lysenin-induced pore formation are 10−67% of the average values when two to three independent experiments are conducted for each lysenin concentration using 10−20 single GUVs in each independent experiment (Figure 7B). Thereby, the rate constants of lysenin-induced pore formation have only one significant digit. Hence, it is possible to compare only large differences in rate constants of pore formation. Recently, inhomogeneity in lipid composition was observed in single nanoscale liposomes using fluorescent probe-labeled lipids.[51] The inhomogeneity in lipid composition, i.e., the fluctuation of the number of constituent lipids, greatly decreased with an increase in the diameter of liposomes, i.e., the total number of lipids in the membrane of single liposomes,[51] as expected from the statistical physics.[52] However, a small inhomogeneity in the lipid composition exists in single GUVs with multiple components. Fluctuation of the lipid composition such as SM concentration in the membrane of single GUVs may be one of the important factors contributing to the large standard errors of the membrane permeability coefficients and the rate constants of pore formation. In the future, a more systematic study of the inhomogeneity of lipid compositions of single GUVs with diameters of 10−30 μm used in the single-GUV method is needed. Moreover, if we could improve the single-GUV method to allow examination of a much larger number of single GUVs, the number of significant digits of these rate constants would increase.

CONCLUSION

Using the single-GUV method, we succeed in determining the rate constants of lysenin-induced pore formation in lipid membranes (k_P) and also the membrane permeability coefficient of a fluorescent probe through the lysenin-induced pores. We found that there was a strong correlation between the P^s values and the SDS-resistant oligomer fraction of lysenin in SM/DOPC (58/42) and SM/DOPC/chol (42/30/28) membranes, indicating that the pore concentration in lipid membranes increases with an increase in the level of the SDS-resistant oligomer of lysenin. We also found that lysenin formed pores in GUVs with SM/chol (60/40) membranes in the homogeneous liquid-ordered phase without disruption of GUVs, indicating that the phase boundary is not necessary for pore formation. However, the P^s values and the SDS-resistant oligomer fractions of lysenin of SM/chol (60/40) membranes indicate that not all of the oligomers in the membrane can convert into pores; i.e., there are irreversible oligomers (or prepores) before conversion to pores. These data provide valuable information about the elementary processes of lysenin-induced pore formation in lipid membranes.

ASSOCIATED CONTENT

Supporting Information

Experimental data of membrane permeation of AF-SBTI from single SM/DOPC/chol (42/30/28) GUVs induced by lysenin and membrane permeation of calcein from single SM/DOPC (90/10) GUVs induced by lysenin. This material is available free of charge via the Internet at http://pubs.acs.org.

AUTHOR INFORMATION

Corresponding Author

*Integrated Bioscience Section, Graduate School of Science and Technology, Shizuoka University, 836 Oya, Suruga-ku, Shizuoka 422-8529, Japan. Telephone and fax: 81-54-238-4741. E-mail: spmyama@ipc.shizuoka.ac.jp.

Funding

This work was supported in part by a Grant-in-Aid for Scientific Research (B) (21310080) from the Japan Society for the Promotion of Science (JSPS) to M.Y.

Notes

The authors declare no competing financial interest.

ACKNOWLEDGMENTS

We greatly appreciate the contributions of Ms. Yuko Saga and Ms. Rei Takagi to preliminary experiments during this work. This work was partially conducted using instruments at the Center for Instrumental Analysis of Shizuoka University.

REFERENCES

(1) Heuck, A. P., Tweten, R. K., and Johnson, A. E. (2001) *β*-Barrel pore-forming toxins: Intriguing dimorphic proteins. *Biochemistry 40*, 9065−9073.

(2) Parker, M. W. (2003) Cryptic clues as to how water-soluble protein toxins form pores in membranes. *Toxicon 42*, 1−6.

(3) Parker, M. W., and Feil, S. C. (2005) Pore-forming protein toxins: From structure to function. *Prog. Biophys. Mol. Biol. 88*, 91−142.

(4) Anderluh, G., and Lakey, J. (2010) *Proteins: Membrane binding and pore formation*, Springer-Verlag, Berlin.

(5) Tomita, T., Watanabe, M., and Yasuda, T. (1992) Influence of membrane fluidity on assembly of *Staphylococcus aureus* *α*-toxin, a channel-forming protein, in liposome membrane. *J. Biol. Chem. 267*, 13391−13397.

(6) Tilley, S. J., Oriova, E. V., Gilbert, R. J. C., Andrew, P. W., and Saibll, H. R. (2005) Structural basis of pore formation by the bacterial toxin pneumolysin. *Cell 121*, 247−256.

(7) Kristant, K., Podlesek, Z., Hojink, V., Gutierrez-Anderluh, I., Guncar, G., Turk, D., Gonzalez-Manas, J. M., Lakey, J. H., Macek, P., and Anderluh, G. (2004) Pore formation by equinatoxin, a eukaryotic pore-forming toxin, requires a flexible N-terminal region and a stable *β*-sandwich. *J. Biol. Chem. 279*, 46509−46517.

(8) Yamaji, A., Sekizawa, Y., Emoto, K., Sakurabe, H., Inoue, K., Kobayashi, H., and Umeda, M. (1998) Lysenin, a novel sphingomyelin-specific binding protein. *J. Biol. Chem. 273*, 5300−5306.

(9) Yamaji-Hasegawa, A., Makino, A., Baba, T., Senoh, Y., Kimura, H., Sato, S. B., Terada, N., Ohno, S., Kiyokawa, E., Umeda, M., and Kobayashi, T. (2003) Oligomerization and pore formation of a sphingomyelin-specific toxin, lysenin. *J. Biol. Chem. 278*, 22762−22770.

(10) Ishitsuka, R., Yamaji-Hasegawa, A., Hirabayashi, A. Y., and Kobayashi, T. (2004) A lipid-specific toxin reveals heterogeneity of sphingomyelin-containing membranes. *Biophys. J. 86*, 296−300.

(11) Ishitsuka, R., and Kobayashi, T. (2007) Cholesterol and lipid/protein ratio control the oligomerization of a sphingomyelin-specific toxin, lysenin. *Biochemistry 46*, 1495−1502.

(12) Kulma, M., Herec, M., Grudzinski, W., Anderluh, G., Gruszecki, W. I., Kwiatkowska, K., and Sobota, A. (2010) Sphingomyelin-rich domains are sites of lysenin oligomerization: Implications for raft studies. *Biochim. Biophys. Acta 1798*, 471−481.

(13) Evans, E., and Rawicz, E. (1990) Entropy-driven tension and bending elasticity in condensed-fluid membranes. *Phys. Rev. Lett. 64*, 2094−2097.

(14) Farge, E., and Devaux, P. F. (1992) Shape changes of giant liposomes induced by an asymmetric transmembrane distribution of phospholipids. *Biophys. J. 61*, 347−357.

(15) Saitoh, A., Takiguchi, K., Tanaka, Y., and Hotani, H. (1998) Opening-up of liposomal membranes by talin. *Proc. Natl. Acad. Sci. U.S.A. 95*, 1026−1031.

(16) Zhao, H., Mattila, J.-P., Holopainen, J. M., and Kinnunen, P. K. J. (2001) Comparison of the membrane association of two antimicrobial peptides, magainin 2 and indolicidin. *Biophys. J. 81*, 2979−2991.

(17) Zhao, H., Rinaldi, A. C., Giulio, A. D., Simmaco, M., and Kinnunen, P. K. J. (2002) Interactions of the antimicrobial peptides temporins with model biomembranes. Comparison of temporins B and L. *Biochemistry 41*, 4425−4436.

(18) Tanaka, T., Tamba, Y., Masum, S. M., Yamashita, Y., and Yamazaki, M. (2002) La^{3+} and Gd^{3+} induce shape change of giant unilamellar vesicles of phosphatidylcholine. *Biochim. Biophys. Acta 1564*, 173−182.

(19) Yamashita, Y., Masum, S. M., Tanaka, T., and Yamazaki, M. (2002) Shape changes of giant unilamellar vesicles of phosphatidylcholine induced by a de novo designed peptide interacting with their membrane interface. *Langmuir 18*, 9638−9641.

(20) Yamazaki, M. (2008) The single GUV method to reveal elementary processes of leakage of internal contents from liposomes induced by antimicrobial substances. In *Advances in Planar Lipid Bilayers and Liposomes* (Leitmannova, A. L., Ed.) Vol. 7, pp 121−142, Elsevier/Academic Press, London.

(21) Tamba, Y., Ohba, S., Kubota, M., Yoshioka, H., Yoshioka, H., and Yamazaki, M. (2007) Single GUV method reveals interaction of tea catechin (−)-epigallocatechin gallate with lipid membranes. *Biophys. J. 92*, 3178−3194.

(22) Tanaka, T., and Yamazaki, M. (2004) Membrane fusion of giant unilamellar vesicles of neutral phospholipid membranes induced by La^{3+}. *Langmuir 20*, 5160−5164.

(23) Tanaka, T., Sano, R., Yamashita, Y., and Yamazaki, M. (2004) Shape changes and vesicle fission of giant unilamellar vesicles of liquid-ordered phase membrane induced by lysophosphatidylcholine. *Langmuir 20*, 9526−9534.

(24) Inaoka, Y., and Yamazaki, M. (2007) Vesicle fission of giant unilamellar vesicles of liquid-ordered phase-membranes induced by amphiphiles with a single long hydrocarbon chain. *Langmuir 23*, 720−728.
(25) Tamba, Y., and Yamazaki, M. (2005) Single giant unilamellar vesicle method reveals effect of antimicrobial peptide, magainin-2, on membrane permeability. *Biochemistry 44*, 15823−15833.
(26) Tamba, Y., and Yamazaki, M. (2009) Magainin 2-induce pore formation in the lipid membranes depends of its concentration in the membrane interface. *J. Phys. Chem. B 113*, 4846−4852.
(27) Tamba, Y., Ariyama, H., Levadny, V., and Yamazaki, M. (2010) Kinetic pathway of antimicrobial peptide magainin 2-induced pore formation in lipid membranes. *J. Phys. Chem. B 114*, 12018−12026.
(28) Tamba, Y., Tanaka, T., Yahagi, T., Yamashita, Y., and Yamazaki, M. (2004) Stability of giant unilamellar vesicles and large unilamellar vesicles of liquid-ordered phase membranes in the presence of Triton X-100. *Biochim. Biophys. Acta 1667*, 1−6.
(29) Maeda, T., and Ohnishi, S. (1980) Activation of influenza virus by acidic media causes hemolysis and fusion of erythrocytes. *FEBS Lett. 122*, 283−287.
(30) Yamazaki, M., and Ito, T. (1990) Deformation and instability in membrane structure of phospholipid vesicles caused by osmophobic association: Mechanical stress model for the mechanism of poly (ethylene glycol)-induced membrane fusion. *Biochemistry 29*, 1309−1314.
(31) Yamashita, Y., Oka, M., Tanaka, T., and Yamazaki, M. (2002) A mew method for preparation of giant liposomes in high salt concentrations and growth of protein microcrystals in them. *Biochim. Biophys. Acta 1561*, 129−134.
(32) Tamba, Y., Terashima, H., and Yamazaki, M. (2011) A membrane filtering method for the purification of giant unilamellar vesicles. *Chem. Phys. Lipids 164*, 351−358.
(33) Yamazaki, M., Ohnihi, S., and Ito, T. (1989) Osmoelastic coupling in biological structures: Decrease in membrane fluidity and osmophobic association of phospholipid vesicles in response to osmotic stress. *Biochemistry 28*, 3710−3715.
(34) Rasband, W. S. (1997−2011) *ImageJ*, version 1.45s, National Institutes of Health, Bethesda, MD (http://imagej.nih.gov/ij/).
(35) Yoshida, N., Tamura, M., and Kinjo, M. (2000) Fluorescence correlation spectroscopy: A new tool for probing the microenvironment of the internal space of organelles. *Single Mol. 1*, 279−283.
(36) Gribbon, P., and Hardingham, T. E. (1998) Macromolecular diffusion of biological polymers measured by confocal fluorescence recovery after photobleaching. *Biophys. J. 75*, 1032−1039.
(37) Baumgard, T., Hess, S. T., and Webb, W. W. (2003) Imaging coexisting fluid domains in biomembranes models coupling curvature and line tension. *Nature 425*, 821−824.
(38) Kwiatkowska, K., Hordejuk, R., Szymczyk, P., Kulma, M., Abdel-Shakor, A., Plucienniczak, A., Dolowy, K., Szewczyk, A., and Sobota, A. (2007) Lysenin-His, a sphingomyelin-recognizing toxin, requires tryptophan 20 for cation-selective channel assembly but not membrane binding. *Mol. Membr. Biol. 24*, 121−134.
(39) Miller, C., Ed. (1986) *Ion channel reconstitution*, Plenum Press, New York.
(40) Bayley, H., Jayasinghe, L., and Wallace, M. (2005) Prepore for a breakthrough. *Nat. Struct. Mol. Biol. 12*, 385−386.
(41) Lawrence, J. C., Saslowsky, D. E., Edwardson, J. M., and Henderson, R. M. (2003) Real-time analysis of the effects of cholesterol on lipid raft behavior using atomic force microscopy. *Biophys. J. 84*, 1827−1832.
(42) Aoki, T., Hirano, M., Takeuchi, Y., Kobayashi, T., Yanagida, T., and Ide, T. (2010) Single channel properties of lysenin measured in artificial lipid bilayers applications to biomolecule detection. *Proc. Jpn. Acad., Ser. B 86*, 920−925.
(43) Doi, M. (1996) *Introduction to Polymer Physics*, Oxford University Press, Oxford, U.K.
(44) Mabrey, S., and Sturtevant, J. M. (1976) Investigation of phase transitions of lipids and lipid mixtures by high sensitivity differential scanning calorimetry. *Proc. Natl. Acad. Sci. U.S.A. 73*, 3862−3866.
(45) Veatch, S. L., and Keller, S. L. (2005) Seeing spots: Complex phase behavior in simple membranes. *Biochim. Biophys. Acta 1746*, 172−185.
(46) Döbereiner, H.-G., Käs, J., Noppl, D., Sprenger, I., and Sackmann, E. (2003) Budding and fission of vesicles. *Biophys. J. 65*, 1396−1403.
(47) Marsh, D. (1996) Lateral pressure in membranes. *Biochim. Biophys. Acta 1286*, 183−223.
(48) Needham, D., and Nunn, R. S. (1990) Elastic deformation and failure of lipid bilayer membranes containing cholesterol. *Biophys. J. 58*, 997−1009.
(49) Simons, K., and Toomre, D. (2000) Lipid rafts and signal transduction. *Nat. Rev. Mol. Cell Biol. 1*, 31−40.
(50) Schön, P., Garcia-Saez, A. J., Malovrh, P., Bacia, K., Anderluh, G., and Schwille, P. (2008) Equinatoxin II permeabilizing activity depends on the presence of sphingomyelin and lipid coexistence. *Biophys. J. 95*, 691−698.
(51) Larsen, J., Hatzakis, N. S., and Stamou, D. (2011) Observation of inhomogeneity in the lipid composition of individual nanoscale liposomes. *J. Am. Chem. Soc. 133*, 10685−10687.
(52) Landau, L. D., and Lifshitz, E. M. (1980) *Statistical Physics*, 3rd ed., Vol. 5, Part 1, Butterworth-Heinmann, Oxford, U.K.